

Rotation Profiles of Solar-like Stars with Magnetic Fields *

Wu-Ming Yang¹ and Shao-Lan Bi^{2,3}

¹ Department of Physics and Chemistry, Henan Polytechnic University, Jiaozuo 454000, China;
wuming.yang@hotmail.com

² Department of Astronomy, Beijing Normal University, Beijing 100875, China

³ National Astronomical Observatories/Yunnan Observatory, Chinese Academy of Sciences, Kunming 650011, China

Received 2007 December 17; accepted 2008 May 14

Abstract We investigate the rotation profile of solar-like stars with magnetic fields. A diffusion coefficient of magnetic angular momentum transport is deduced. Rotating stellar models with different mass incorporating the coefficient are computed to give the rotation profiles. The total angular momentum of a solar model with only hydrodynamic instabilities is about 13 times larger than that of the Sun at the age of the Sun, and this model can not reproduce quasi-solid rotation in the radiative region. However, the solar model with magnetic fields not only can reproduce an almost uniform rotation in the radiative region, but also a total angular momentum that is consistent with the helioseismic result at the 3σ level at the age of the Sun. The rotation of solar-like stars with magnetic fields is almost uniform in the radiative region, but for models of $1.2\text{--}1.5 M_{\odot}$, there is an obvious transition region between the convective core and the radiative region, where angular velocity has a sharp radial gradient, which is different from the rotation profile of the Sun and of massive stars with magnetic fields. The change of angular velocity in the transition region increases with increasing age and mass.

Key words: stars: evolution — stars: rotation — stars: magnetic fields

1 INTRODUCTION

Helioseismology has given us detailed information about the internal structure and rotation of the Sun: the Sun's rotation is slow in the core and is almost uniform in the radiative region, but the angular velocity has a latitudinal gradient in the convective zone (Gough et al. 1996; Schou et al. 1998; Chaplin et al. 1999). The inversion data of solar-like stars, though limited, have revealed that localized information of stellar interior can be given by astroseismology (Gough & Kosovichev 1993; Gough 1998; Roxburgh et al. 1998; Berthomieu et al. 2001; Basu et al. 2002; Basu 2003). Furthermore, it has been shown that the localized information on the internal rotation profile of a solar-like star can be obtained from frequencies of oscillations (Gough & Kosovichev 1993; Gough 1998; Goupil et al. 1996; Lochard et al. 2004, 2005). Information on the internal rotation of β Cepheid has already been provided by astroseismology (Aerts et al. 2003). Using the data of the Microvariability and Oscillation of Star (MOST) satellite, Walker et al. (2007) found that kappa-1 Ceti has a differential rotation profile closely resembling that of the Sun. With the ongoing and forthcoming space seismic missions: COvection, ROTatin and planetary Transits (COROT) (Baglin 2006) and Kepler (Christensen-Dalsgaard et al. 2007), it will be possible to extract information on the internal rotation profile of solar-like stars.

Moreover, magnetic fields of active regions on solar surface are believed to be resulted from strong toroidal magnetic fields generated by the solar dynamo at the base of the convective zone. Our understanding

* Supported by the National Natural Science Foundation of China.

of both the stellar magnetic activity and the generation of magnetic fields depends on information about the interior rotational properties of stars (Thompson et al. 2003; Fan 2004; Charbonneau 2005), but the evolution of the rotation profile inside stars is poorly understood, which therefore is important for us to obtain a global picture of how the rotation profile inside stars evolves.

The influence of rotation on the stellar structure and evolution has been studied by many investigators (Kippenhahn & Thomas 1970; Endal & Sofia 1976; Pinsonneault et al. 1989; Meynet & Maeder 1997; Huang et al. 2007). Redistribution of angular momentum within the star's interior has also been considered by many authors (Endal & Sofia 1981; Chaboyer et al. 1995; Maeder & Meynet 2000; Palacios et al. 2003; Huang 2004). These studies show that hydrodynamic transport of angular momentum is rather inefficient inside stars, therefore magnetic angular momentum transport or other mechanisms should be considered in rotating stars. Magnetic angular momentum transport in massive stars has been investigated by Maeder & Meynet (2003, 2004, 2005). The massive stars with magnetic fields rotate almost as a solid body throughout the whole star (Maeder & Meynet 2004). Eggenberger et al. (2005) and Yang & Bi (2006) studied the rotation profile of the Sun and showed that a quasi-solid rotation in the Sun can be achieved by considering the effect of the magnetic fields. In this paper, we mainly focus on the internal rotation profiles of solar-like stars. In Section 2 the diffusion coefficient of magnetic angular momentum transport is given. In Section 3 numerical calculation and results are presented. Lastly, a discussion and conclusions are presented in Section 4.

2 DIFFUSION COEFFICIENT OF MAGNETIC ANGULAR MOMENTUM TRANSPORT

Spruit (1999, 2002) developed the Tayler-Spruit dynamo, which can generate magnetic fields in the radiative region of differentially rotating stars. These fields are predominantly azimuthal components, $B \sim B_\phi$. If magnetic fields exist in stars, magnetic angular momentum transport can be described by magnetic induction and momentum equations. For a constant magnetic diffusivity and shellular rotation (Zahn 1992), assuming axisymmetry and considering only the Lorentz force, the azimuthal components of the induction and momentum equations are (Barnes et al. 1999; Yang & Bi 2006)

$$\frac{\partial B_\phi}{\partial t} + \eta \left(\frac{1}{r^2 \sin^2 \theta} - \nabla^2 \right) B_\phi = r \sin \theta \mathbf{B}_p \cdot \nabla \Omega, \quad (1)$$

$$\rho r^2 \sin^2 \theta \frac{\partial \Omega}{\partial t} = \frac{1}{4\pi} \mathbf{B}_p \cdot \nabla (r \sin \theta B_\phi). \quad (2)$$

If the effect of the magnetic diffusivity is to limit the growth of the toroidal field after some time, the growth of the instability is then halted by dissipative processes that operate on some timescale, τ . Accordingly the second term on the left-hand side of Equation (1) may be replaced simply by B_ϕ/τ (Barnes et al. 1999). Substituting for the second term of Equation (1) and differentiating Equation (1) with respect to time, one then obtains (Barnes et al. 1999)

$$\frac{\partial^2 B_\phi}{\partial t^2} + \frac{1}{\tau} \frac{\partial B_\phi}{\partial t} = r \sin \theta \mathbf{B}_p \cdot \nabla \frac{\partial \Omega}{\partial t}. \quad (3)$$

For much longer time than the timescale of the instability, one would expect the term involving the first time derivative to dominate (Barnes et al. 1999), so we have

$$\frac{1}{\tau} \frac{\partial B_\phi}{\partial t} \approx r \sin \theta \mathbf{B}_p \cdot \nabla \frac{\partial \Omega}{\partial t}. \quad (4)$$

For shellular rotation $\Omega(r, \theta) \sim \Omega(r)$ (Zahn 1992),

$$B_\phi \sim \tau r \sin \theta B_r \frac{\partial \Omega}{\partial r}. \quad (5)$$

Using Equation (5), Equation (2) can be rewritten as

$$\rho r^2 \frac{\partial \Omega}{\partial t} \approx \frac{1}{4\pi \sin^2 \theta} \mathbf{B}_p \cdot \nabla \left(\tau r^2 \sin^2 \theta B_r \frac{\partial \Omega}{\partial r} \right)$$

$$\begin{aligned} &\approx \frac{B_r}{4\pi} \frac{\partial}{\partial r} \left(\tau r^2 B_r \frac{\partial \Omega}{\partial r} \right) \\ &\approx \frac{1}{r^2} \frac{\partial}{\partial r} \left(\frac{\tau B_r^2}{4\pi \rho} r^4 \rho \frac{\partial \Omega}{\partial r} \right). \end{aligned} \quad (6)$$

The diffusion coefficient for angular momentum transport can thus be obtained as

$$D_m = \frac{\tau B_r^2}{4\pi \rho}. \quad (7)$$

In Yang & Bi (2006) we also obtained a similar diffusion coefficient, but it was only an assumption that the coefficient can be used in the equation of the transport of angular momentum. From Equation (6) it can be found that the magnetic angular momentum transport approximately obeys the diffusion coefficient D_m .

For a steady equilibrium, the dissipating timescale τ has to match the growth timescale σ^{-1} of the instability. Using the growth time scale of magnetic instability given by Pitts & Tayler (1985) and Spruit (1999),

$$\sigma^{-1} = \frac{\Omega}{\omega_A^2}, \omega_A = \frac{B_\phi}{(4\pi \rho)^{1/2} r}, \quad (8)$$

one can obtain the diffusion coefficient

$$\begin{aligned} D_m &= \frac{B_r^2}{4\pi \rho} \frac{\Omega}{\omega_A^2} \\ &= r^2 \Omega \left(\frac{B_r}{B_\phi} \right)^2. \end{aligned} \quad (9)$$

Equation (9) can also be rewritten as

$$D_m = r^2 \Omega \left(\frac{\omega_{rA}}{\omega_A} \right)^2, \quad (10)$$

where

$$\omega_{rA} = \frac{B_r}{(4\pi \rho)^{1/2} r}, \quad (11)$$

Equation (10) hints that magnetic angular momentum transport is related to Alfvén waves.

The distribution of magnetic fields inside a star is poorly known. One form was given by Spruit (2002)

$$\frac{B_r}{B_\phi} = q \left(\frac{\Omega}{N_\mu} \right)^2, \quad (12)$$

where $q = -\frac{\partial \ln \Omega}{\partial \ln r}$, for the case (labelled 0) where the effect of thermal diffusion can be neglected, namely $N_\mu > N_T$, and

$$\frac{B_r}{B_\phi} = 2^{1/4} \left(\frac{\Omega}{N_T} \right)^{1/4} \left(\frac{\kappa}{r^2 N_T} \right)^{1/4} \quad (13)$$

for the case (labelled 1) that has the effect of thermal diffusion included. Using Equations (12) and (13), one can rewrite Equation (9) as

$$D_{m0} = r^2 \Omega q^2 \left(\frac{\Omega}{N_\mu} \right)^4 \quad (14)$$

for the case 0 and

$$D_{m1} = 2^{1/2} r^2 \Omega \left(\frac{\Omega}{N_T} \right)^{1/2} \left(\frac{\kappa}{r^2 N_T} \right)^{1/2} \quad (15)$$

for the case 1. Equations (14) and (15) are consistent with the effective magnetic viscosity defined by Spruit (2002) and Maeder & Meynet (2004) for the radial transport of angular momentum. Equations (14) and (15) are only two cases of D_m . The Tayler-Spruit dynamo scenario was validated by Braithwaite (2006), but was contrary to the findings of Zahn et al. (2007). The rotation profile of massive stars with magnetic fields was investigated by Maeder & Meynet (2004), and the rotation profile of the Sun with magnetic fields was studied by Eggenberger et al. (2005). In this work we mainly check solar-like stars with mass $1.0\text{--}1.5 M_\odot$.

Table 1 Model Parameters

Model	Mass M_{\odot}	J_0^a $10^{50} \text{ g cm}^2 \text{ s}^{-1}$	f_k	$f_{\Omega 1}^b$	$f_{\Omega 2}^c$
M1.0a	1.0	1.591	3.0	1.0	0
M1.0b	1.0	1.591	3.0	1.0	0.01
M1.2	1.2	1.9095	3.0	1.0	0.01
M1.4	1.4	1.534	1.0	1.0	0.01
M1.5	1.5	1.095	1.0	1.0	0.01

^a Initial angular momentum;

^b Value of f_{Ω} for the coefficient of hydrodynamic instabilities (Pinsonneault et al. 1989);

^c Value of f_{Ω} for D_m ; model M1.0a with only hydrodynamic instabilities.

3 NUMERICAL CALCULATION AND RESULTS

3.1 Angular Momentum Transport and Loss

The Yale Rotation Evolution Code (YREC7) was used to construct stellar models in its rotating configuration (Pinsonneault et al. 1989; Guenther et al. 1992). All models were evolved from fully convective pre-main sequence (PMS) to somewhere near the end of the Main Sequence (MS). The newest OPAL EOS-2005¹ (Rogers & Nayfonov 2002), OPAL opacity (Iglesias & Rogers 1996), and the opacity for low temperature provided by Alexander & Ferguson (1994) were used. The models take into account diffusion of helium and metals, using the prescription of Thoul et al. (1994). The initial chemical composition of the models is fixed at $Z_0 = 0.02$, $X_0 = 0.706$.

Hydrodynamic instabilities considered in the YREC7 have been presented by Pinsonneault et al. (1989). It is assumed that convection enforces the solid-body rotation in the convective regions of the star, so rotational instabilities are effective only in the radiative regions. The transport of angular momentum is treated using (Endal & Sofia 1978; Pinsonneault et al. 1989)

$$\rho r^2 \frac{\partial \Omega}{\partial t} = f_{\Omega} \frac{1}{r^2} \frac{\partial}{\partial r} \left(\rho r^4 D \frac{\partial \Omega}{\partial r} \right), \quad (16)$$

in the radiative regions of the star, where f_{Ω} is an adjustable parameter introduced to represent some inherent uncertainties in the diffusion equation. In stars with $M \leq 1.5 M_{\odot}$, the angular momentum loss due to magnetic braking is treated using a parameterized formula (Kawaler 1988),

$$\frac{dJ}{dt} = f_K K_{\Omega} \left(\frac{R}{R_{\odot}} \right)^{1/2} \left(\frac{M}{M_{\odot}} \right)^{-1/2} \Omega^3, \quad (17)$$

to reproduce the Skumanich relationship (Skumanich 1972), where $K_{\Omega} \simeq 1.13 \times 10^{47} \text{ g cm}^2 \text{ s}$, and f_K is an adjustable parameter. It is assumed that magnetic braking has an effect on the whole convective envelope. In some case, a PMS star extracts angular momentum from the star as well as supplies angular momentum to the star (Stassun & Terndrup 2003). Moreover, it has been argued by Matt & Pudritz (2005a, b) that the spin-down of PMS stars may not be due to a magnetic star-disk interaction, but may result from a magnetic stellar wind. Thus for simplicity, we do not consider the magnetic star-disk interaction.

The initial angular momentum of a star is still uncertain. Kawaler (1987) showed that the angular momentum J of stars more massive than $1.5 M_{\odot}$ is proportional to squared mass M^2 , but the mass-momentum relation of stars below $1.5 M_{\odot}$ is uncertain. As a first trial, we take the initial angular momentum to be a free parameter. The adjustable parameters mentioned above are listed in Table 1.

3.2 Results of Calculation

Figure 1 compares the evolution of the internal rotation profile of two $1.0 M_{\odot}$ models, one with only the hydrodynamic instabilities given by Pinsonneault et al. (1989) and one with both the hydrodynamic instabilities and magnetic fields. Both models are evolved from PMS with initial angular momentum $J_0 = 1.591 \times 10^{50} \text{ g cm}^2 \text{ s}^{-1}$ at age of 4.5 Gyr. During the PMS phase, although with angular momentum

¹ <http://physci.llnl.gov/Research/OPAL/>

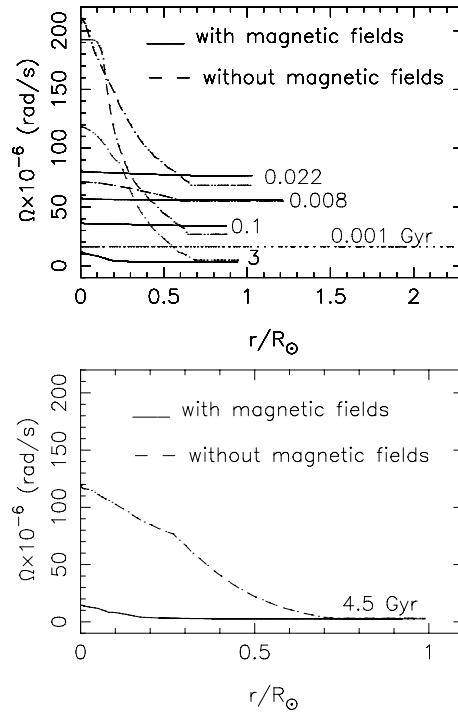


Fig. 1 Rotation profiles as a function of radius for $1.0 M_{\odot}$ model at different ages labeled by Gyr. Top panel shows the rotation profiles of models M1.0a and M1.0b at different ages. Bottom panel displays the distribution of angular velocity of the models at age 4.5 Gyr. The initial angular momentum $J_0 = 1.591 \times 10^{50} \text{ g cm}^2 \text{ s}^{-1}$. The dotted line indicates the solid-body rotation of the models with and without magnetic fields on the pre-main sequence.

loss from the surface of models, the rotation rate rapidly increases due to the fast contraction. The internal rotation profile of the model with magnetic fields is different from that of the model with only hydrodynamic instabilities when the models are near the zero-age main sequence (ZAMS). The model with only hydrodynamic instabilities has a fast rotation core. The rotation of the model with magnetic fields is, however, almost uniform. During the early stage of the MS, the rotation of the model M1.0a is differential rotation, while the model M1.0b is a quasi-solid body rotation. At the age of 4.5 Gyr, the surface rotation rates of the two models are around $2.7 \times 10^{-6} \text{ rad s}^{-1}$. However, the internal distribution of angular velocity is quite different. The model M1.0a shows a strong differential rotation with a factor of about 40 between the angular velocity in the core and at the surface, while the model M1.0b shows an almost uniform angular velocity, with a small increase in $\Omega(r)$ in the center ($r < 0.2 R_{\odot}$), see Eggenberger et al. (2005). The surface rotation rate is higher in M1.0b than in M1.0a in the early evolutionary stage, and the loss rate of angular momentum is related to Ω^3 . Consequently, the angular momentum loss of model is higher in M1.0b than in M1.0a. The total angular momentum of model M1.0a is $2.628 \times 10^{49} \text{ g cm}^2 \text{ s}^{-1}$ at age 4.5 Gyr, which is about 13 times larger than the seismic result $(1.94 \pm 0.05) \times 10^{48} \text{ g cm}^2 \text{ s}^{-1}$ (Komm et al. 2003), while the total angular momentum of model M1.0b is $2.045 \times 10^{48} \text{ g cm}^2 \text{ s}^{-1}$ at the same age, which is consistent with the result of helioseismology at the level of 3σ .

Figure 2 shows the evolution of the internal rotation profile of model M1.2. In the early evolutionary stage, the angular velocity $\Omega(r)$ is almost constant. At the stage of $X_c \sim 0.69$, about 90% of the initial angular momentum has been lost, and the rotation is nearly uniform in the radiative region, but the rotation of the convective core is faster than that of the radiative region. There is a transition region between the two, where the angular velocity has a sharp radial change due to the spin-down of the outer parts resulting from angular momentum loss, and a decrease of the horizontal coupling provided by the magnetic field

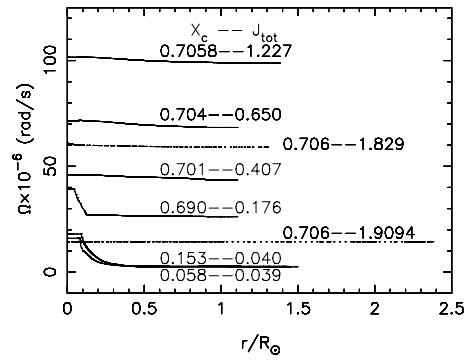


Fig. 2 Rotation profiles as a function of radius for model M1.2 at the different evolutionary stages indicated by the central hydrogen X_c . The initial angular momentum $J_0 = 1.9095 \times 10^{50} \text{ g cm}^2 \text{ s}^{-1}$, J_{tot} is the total angular momentum of models in $10^{50} \text{ g cm}^2 \text{ s}^{-1}$. The lower dotted line shows the rotation profile of PMS model at age of 1 Myr.

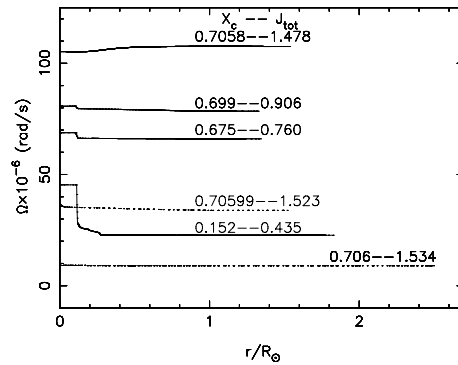


Fig. 3 Same as Fig. 2 but for model M1.4. The initial angular momentum $J_0 = 1.534 \times 10^{50} \text{ g cm}^2 \text{ s}^{-1}$.

resulting from an increase in μ -gradient in the region. The loss of angular momentum mainly occurs in the early evolutionary stage. During the late stage of the MS, the total angular momentum of model M1.2 is only a few percent of the initial angular momentum, and the rotation is slow, thus the loss rate of angular momentum is very low. Consequently, the angular momentum of model M1.2 is almost conserved from the stage of $X_c = 0.153$ to the stage of $X_c = 0.058$.

The evolutions of the internal rotation profiles of models M1.4 and M1.5 are shown in Figures 3 and 4, respectively. The model M1.4 has lost about 50% of the initial angular momentum at the stage of $X_c = 0.675$, while the model M1.5 has only lost about 15% of the initial angular momentum even at the stage of $X_c = 0.487$. Distributions of the angular velocity of models M1.4 and M1.5 are different from that of model M1.2. The angular velocity between the convective core and the radiative region of models M1.4 and M1.5 decreases obviously when the radius increases. The radial change of the angular velocity between the convective core and the radiative region in models M1.4 and M1.5 is larger than that in model M1.2, which should be due to the μ -gradient and the fast spin-down occurring at the same stage in models M1.4 and M1.5. However, in model M1.2, the fast spin-down occurs in the early evolutionary stage when the μ -gradient is small.

Figure 5 shows the distribution of the hydrogen mass fraction X of models M1.2 and M1.4. It is obvious that there is a sharp μ -gradient at the bottom of the radiative region of models M1.2 and M1.4 at the late stage of MS. The μ -gradient and the Ω -gradient are in the same region. The ratio of magnetic

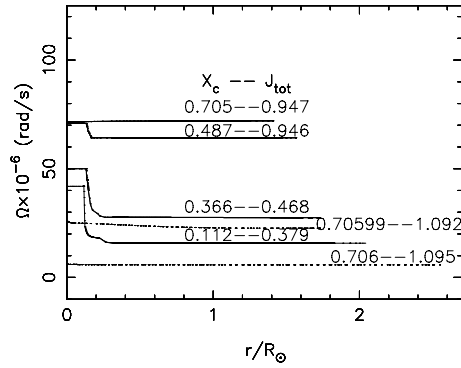


Fig. 4 Same as Fig. 2 but for model M1.5. The initial angular momentum $J_0 = 1.095 \times 10^{50} \text{ g cm}^2 \text{ s}^{-1}$.

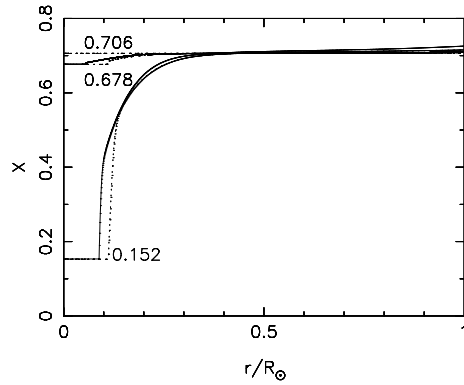


Fig. 5 Internal distribution of the hydrogen mass fraction X as a function of the radius. The solid lines show the model M1.2, and dotted lines refer to model M1.4.

field, B_r/B_ϕ , is related to ∇_μ^{-1} in the Tayler-Spruit dynamo, namely $D_m \sim \nabla_\mu^{-2}$. Thus the increase in μ -gradient must lead to the decrease in the coupling provided by magnetic fields. This scenario was first found by Eggenberger et al. (2005) in the Sun.

4 DISCUSSION AND CONCLUSIONS

The surface velocity is sensitive to the loss rate of the angular momentum. Equation (17) may overestimate the loss rate of angular momentum of the rapid rotation stars (Andronov et al. 2003), but it can reproduce the Sun's rotation, so we take it in our models. The adjustable parameter, f_k , is adjusted to obtain the solar rotation rate at age of 4.5 Gyr in models M1.0a and M1.0b. However, the same value of f_k cannot be applied to models M1.4 and M1.5 because their convective envelope is too shallow, therefore we take a small f_k for models M1.4 and M1.5.

The value of the parameter $f_{\Omega 2}$ is adjusted to obtain a quasi-solid rotation in our models. The value of 0.01 will work in our models, but it is far less than 1. This could be a consequence of overestimating the ratio of B_r to B_ϕ in the Tayler-Spruit dynamo.

The distribution of angular velocity of models M1.0a and M1.0b shows that the rotation profile strongly depends on the efficiency of angular momentum transport. The angular momentum is effectively transported outward by magnetic fields in M1.0b. Thus the rotation of the core of M1.0b is slow compared to M1.0a. The surface rotation rate mainly depends on the loss rate of angular momentum and the amount of outward transport of angular momentum. Because both M1.0a and M1.0b have same values of f_k and initial Ω , the difference in the surface velocity between the two depends on the efficiency of the outward transport of

angular momentum. In M1.0b, the loss of angular momentum is counteracted by magnetic angular momentum transport. Therefore, the surface velocity of M1.0b is higher than that of M1.0a when the interior of M1.0b has enough angular momentum to transport outward. The loss rate of angular momentum is related to Ω^3 , and the amount of angular momentum loss of model M1.0b is larger than that of model M1.0a. This scenario takes place in the early evolutionary stage.

At the early stage of M1.2, the fast spin-down leads to a sharp radial gradient of angular velocity at the top of the convective core, but at the same stage of models M1.4 and M1.5, the spin-down is slow. At the late evolutionary stage of M1.2, although there is a large μ -gradient at the top of the core, the spin-down is very slow. The radial change of the angular velocity is then small compared to that of models M1.4 and M1.5 at the top of the core. However, in models M1.4 and M1.5, the μ -gradient and the fast spin-down resulting from angular momentum loss and stellar expansion occur at the same stage. Therefore, the radial change of angular velocity is large at the top of the core in models M1.4 and M1.5.

The $1.0 M_{\odot}$ model with only hydrodynamic instabilities has a fast rotation core, and its total angular momentum is $2.628 \times 10^{49} \text{ g cm}^2 \text{ s}^{-1}$ at age of 4.5 Gyr, which disagrees with the helioseismic results. In contrast, the $1.0 M_{\odot}$ model with magnetic fields has a slow rotation core, and the rotation is almost uniform in the radiative region, and these features are consistent with the seismic results. Moreover, the total angular momentum of the model with magnetic fields is $2.045 \times 10^{48} \text{ g cm}^2 \text{ s}^{-1}$ at age of 4.5 Gyr, which agrees with the helioseismic result at the 3σ level.

A diffusion coefficient of magnetic angular momentum transport is obtained. It is found not only can the magnetic field reproduce a quasi-solid rotation, but it can also enhance the loss rate of angular momentum. The rotation of solar-like stars with magnetic fields is almost uniform in the radiative regions, this is consistent with the results of helio- and astroseismology. However, there is a transition region between the convective core and the radiative region, where the angular velocity has a sharp radial gradient, which is different from that of solar model and that of massive stars as given by Maeder & Meynet (2004). Moreover, the change of angular velocity in the transition region increases with increasing age and mass.

Acknowledgements This work was supported by the Ministry of Science and Technology of the People's Republic of China through Grant 2007CB815406, and by the NSFC through Grants 10173021, 10433030, 10773003 and 10778601.

References

- Aerts C., Dazynska J., Scuflaire R. et al., 2003, *Sci*, 300, 1926
 Alexander D. R., Ferguson J. W., 1994, *ApJ*, 437, 846
 Andronov N., Pinsonneault M., Sills A., 2003, *ApJ*, 582, 358
 Baglin A., Michel E., Auvergne M. et al., 2006, In: K. Fletcher, M. Thompson, ed., *Proceeding of SOHO 18/GONG 2006/HELAS I, Beyond the spherical Sun*, ESA SP-624, p.34
 Barnes G., Charbonneau P., MacGregor K. B., 1999, *ApJ*, 511, 466
 Basu S., 2003, *Ap&SS*, 284, 153
 Basu S., Christensen-Dalsgaard J., Thompson M. J., 2002, In: F. Favata, I. W. Roxburgh, D. Daladi-Enriquez, ed., *Proc. 1st Eddington Meeting 'Stellar Structure and habitable Planet Finding'*, ESA SP-485, 407
 Berthomieu G., Toutain T., Gonczi G. et al., 2001, In: A. Wilson, ed., *Proc. SOHO 10/GONG 2000 Workshop: Helio- and Asteroseismology at the Dawn of the Millennium*, ESA SP-464, 411
 Braithwaite J., 2006, *A&A*, 449, 451
 Chaboyer B., Demarque P., Pinsonneault M. H., 1995, *ApJ*, 441, 865
 Chaplin W. J., Christensen-dalsgaard J., Elsworth Y. et al., 1999, *MNRAS*, 308, 405
 Charbonneau P., 2005, *LRSP*, 2, 2
 Christensen-Dalsgaard J., Arentoft T., Brown T. M. et al., 2007, *CoAst*, 150, 350
 Eggenberger P., Maeder A., Meynet G., 2005, *A&A*, 440, L9
 Endal A. S., Sofia S., 1976, *ApJ*, 210, 184
 Endal A. S., Sofia S., 1978, *ApJ*, 220, 279
 Endal A. S., Sofia S., 1981, *ApJ*, 243, 625
 Fan Y., 2004, *LRSP*, 1, 1

- Gough D. O., 1998, In: H. Kjeldsen, T.R. Bedding, eds., *The First MONS Workshop: Science with a Small Space Telescope*, Aarhus University: p.33
- Gough D. O., Kosovichev A. G., 1993, *ASPC*, 40, 541
- Gough D. O., Kosovichev A. G., Toomre J. et al., 1996, *Sci*, 272, 1296
- Goupil M. J., Dziembowski W. A., Goode P. R. et al., 1996, *A&A*, 305, 487
- Guenther D. B., Demarque P., Kim Y. C. et al., 1992, *ApJ*, 387, 372
- Huang R. Q., 2004, *A&A*, 422, 981
- Huang R. Q., Song H. F., Bi S. L., 2007, *Chin. J. Astron. Astrophys. (ChJAA)*, 7, 235
- Iglesias C., Rogers F. J., 1996, *ApJ*, 464, 943
- Kawaler S. D., 1987, *PASP*, 99, 1322
- Kawaler S. D., 1988, *ApJ*, 333, 236
- Kippenhahn R., Thomas H. C., In *Stellar Rotation* (Slettebak, A., ed), New York: Gordon and Breach, 1970, p.20
- Komm R., Howe R., Durney B. R. et al., 2003, *ApJ*, 586, 650
- Lochard J., Samadi R., Goupil M. J., 2004, *SoPh.*, 220, 199
- Lochard J., Samadi R., Goupil M. J., 2005, *A&A*, 438, 939
- Maeder A., Meynet G., 2000, *ARA&A*, 38, 43
- Maeder A., Meynet G., 2003, *A&A*, 411, 543
- Maeder A., Meynet G., 2004, *A&A*, 422, 225
- Maeder A., Meynet G., 2005, *A&A*, 440, 104
- Matt S., Pudritz R. E., 2005a, *MNRAS*, 356, 167
- Matt S., Pudritz R. E., 2005b, *ApJ*, 632, L135
- Meynet G., Maeder A., 1997, *A&A*, 321, 465
- Palacios A., Talon S., Charbonnel C. et al., 2003, *A&A*, 399, 603
- Pinsonneault M. H., Kawaler S. D., Sofia S. et al., 1989, *ApJ*, 338, 424
- Pitts E., Tayler R. J., 1985, *MNRAS*, 216, 139
- Rogers F. J., Nayfonov A., *ApJ*, 2002, 576,1064
- Roxburgh I. W., Audard N., Basu S. et al., 1998, In: J. Provost and F. X. Schmider, eds., *Proc. IAU Symp. 181: Sounding Solar and Stellar Interiors*, Nice Observatory, 245
- Schou J., Antia H. M., Basu S. et al., 1998, *ApJ*, 505, 390
- Skumanish A., 1972, *ApJ*, 171, 565
- Spruit H. C., 1999, *A&A*, 349, 189
- Spruit H. C., 2002, *A&A*, 381, 923
- Stassun K. G., Terndrup D., 2003, *PASP*, 115, 505
- Thompson M J., Christensen-Dalsgaard J., Miesch M. S. et al., 2003, *ARA&A*, 41, 599
- Thoul A. A., Bahcall J. N., Loeb A., 1994, *ApJ*, 421, 828
- Walker G. A. H., Croll B., Kuschnig R. et al., 2007, *ApJ*, 659, 1611
- Yang W. M., Bi S. L., 2006, *A&A*, 449, 1161
- Zahn J.-P., 1992, *A&A*, 265, 115
- Zahn J.-P., Brun A. S., Mathis S., 2007, *A&A*, 474, 145